

Supporting Information

**2 Diel variation of mercury stable isotope ratios record photoreduction of PM_{2.5}-bound
3 mercury**

5 Qiang Huang^{1,2}, Jiubin Chen^{1,3,*}, Weilin Huang⁴, John R. Reinfelder⁴, Pingqing Fu⁵, Shengliu
6 Yuan¹, Zhongwei Wang¹, Wei Yuan¹, Hongming Cai¹, Hong Ren⁵, Yele Sun⁵ and Li He⁶

⁸ ¹SKLEG, Institute of Geochemistry, CAS, Guiyang 550081, China

⁹ ²SKLOG, Guangzhou Institute of Geochemistry, CAS, Guangzhou 510640, China

¹⁰ ³Institute of Surface-Earth System Science, Tianjin University, 300072, China

¹¹ ⁴Department of Environmental Sciences, Rutgers, The State University of New Jersey, New
¹² Brunswick, NJ 08901, USA

¹³ ⁵LAPC, Institute of Atmospheric Physics, CAS, Beijing 100029, China

¹⁴ ⁶Laboratory of Hebei Institute of Regional Geology and Mineral Resources Survey,
¹⁵ Shijiazhuang 065000, China

17	*Corresponding author.
18	E-mail: jbchen@tju.edu.cn
19	
20	Page S2
21	Page S6
22	Page S7
23	Page S8
24	Page S9
25	Page S13
26	Page S14
27	Page S15
28	Page S16
29	Page S17
30	Page S18
31	Page S19

32 **1. Materials and methods**

33 **1.1 Materials**

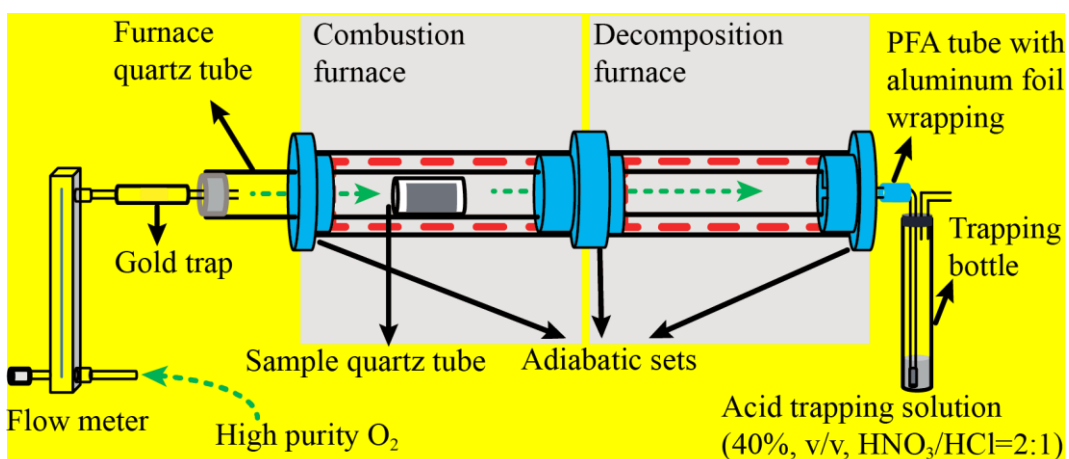
34 HCl, HNO₃ and stannous chloride (SnCl₂) were analytical grade (Sinopharm Chemical
35 Reagent Co., Ltd., China). Milli-Q water (18.2 MΩ, Millipore, USA) was used for preparation
36 all aqueous solutions. Concentrated HCl and HNO₃ were double-distilled using a DST-1000
37 acid purification system (Savillex, USA). Two SnCl₂ solutions of 0.20 and 0.03 g/mL were
38 prepared by dissolving the solid SnCl₂ in 1 M HCl and were used for online reduction of Hg²⁺
39 during the content and isotope measurements, respectively. The National Institute of Standards
40 and Technology Standard Reference Material 3133 (NIST SRM 3133) Hg and UM-Almaden
41 Hg were used as international standards and measured regularly to control the accuracy and
42 quality of isotope analysis. Two other reference materials, the solution NIST SRM 3177 Hg
43 and the Yellow-Red Soil GBW07405 (National Center for Standard Materials, Beijing, China)
44 were used as in-house isotope standards, and were regularly measured for quality control of Hg
45 content and isotope measurements. GBW07405 was also used as procedure standard to evaluate
46 the accuracy and precision of sample pretreatment (Huang et al., 2015; Huang et al., 2016). The
47 NIST SRM 997 Thallium (20 ng mL⁻¹ Tl in 3 % HNO₃) was employed as an internal standard
48 for mass bias correction.

49

50 **1.2 Sample pretreatment for mercury isotopes analysis**

51 After collection, mercury bound on PM_{2.5} with sufficient mass for isotopic analysis ($\geq 10 \text{ ng}$)
52 was concentrated into a 5-mL 40% acid mixture (2:4:9 volumetric ratio of 10 M HCl, 15 M
53 HNO₃ and Milli-Q water) according to the methods reported in Huang et al. (2015). Schematic
54 diagram of the combustion-trapping assembly from Huang et al. (2015) is shown below. To

55 extract Hg bound to PM samples, each filter was rolled into a cylinder and placed in a sample
56 quartz tube. Both ends of the tube were capped with quartz wool (pre-cleaned at 500°C) to
57 prevent particle emission. Each tube was combusted over 2 h in a temperature-programmed
58 dual-stage quartz tube combustion furnace in which the temperature of the first furnace was
59 incrementally increased to 900°C whereas the second furnace was held at 950°C. The resulting
60 Hg vapor was swept by O₂ gas (Hg free) into the 40% acid trapping solution. The trapping
61 solution was diluted with Milli-Q H₂O to 10 mL to a final acid concentration of 20%. The
62 accuracy and precision of the dual-stage combustion protocol were evaluated by the analysis of
63 the GBW07405 using the same digestion method. The detection limit given by the procedural
64 blanks (< 0.3 ng) for this dual-stage combustion method was negligibly low compared to the
65 total Hg mass (≥ 10 ng) extracted from either PM_{2.5} samples or procedural standards.



67 Schematic diagram of the combustion-trapping assembly from Huang et al. (2015).

68

69 **1.3 Mercury concentration and stable isotope composition measurements**

70 The methods used to measure the Hg content and isotope ratio were published elsewhere
71 (Huang et al., 2015). In brief, a small fraction of each trapping solution (20% acid mixture) was
72 used to measure the Hg content on cold-vapor atomic fluorescence spectroscopy (CVAFS,

73 Tekran 2500, Tekran® Instruments Corporation, CA), with a precision better than 10%. The
74 recoveries of Hg for the standard GBW07405 were in the acceptable range of 95 to 105% with
75 an average value of 98% (1 SD = 6%, n = 6); but no recovery of Hg for the PM_{2.5} samples was
76 determined due to limited availability of the samples.

77 A total of 61 PM_{2.5} samples were collected during the sampling campaign. After analysis
78 of Hg contents, we found that 56 PM_{2.5} samples (including 26 daytime and 30 nighttime samples)
79 have sufficient Hg mass and hence were further analyzed for Hg isotope compositions using a
80 multicollector inductively coupled plasma mass spectrometer (MC-ICP-MS, Nu Instruments
81 Ltd., UK) equipped with a continuous flow cold vapor generation system. Detailed protocols
82 for the Hg isotope analysis can be found in Huang et al. (2015). The Faraday cups were
83 positioned to simultaneously collect five Hg isotopes and two Tl isotopes including ²⁰⁵Tl (H3),
84 ²⁰³Tl (H1), ²⁰²Hg (Ax), ²⁰¹Hg (L1), ²⁰⁰Hg (L2), ¹⁹⁹Hg (L3), and ¹⁹⁸Hg (L4). ¹⁹⁶Hg and ²⁰⁴Hg
85 were not measured due to their very low abundance. Instrumental mass bias was corrected using
86 an internal standard (NIST SRM 997 Tl) and strict sample-standard bracketing with NIST SRM
87 3133 Hg standard. For quality assurance and control, the well-known reference material UM-
88 Almaden and the NIST SRM 3177 Hg were inserted repeatedly into the sampling list after every
89 ten and five real samples, measured regularly during sample analysis session, and calibrated
90 periodically against the NIST SRM 3133 Hg as well as samples.

91 Delta (δ) notation is used to represent MDF in units of per mil (‰) as defined by the
92 following equation (Blum and Bergquist, 2007):

$$\delta^x\text{Hg} (\text{\textperthousand}) = [(^x\text{Hg}/^{198}\text{Hg})_{\text{sample}} / (^x\text{Hg}/^{198}\text{Hg})_{\text{NIST3133}} - 1] \times 1000 \quad (1)$$

93 where x = 199, 200, 201, and 202. MIF is reported as the deviation of a measured delta value
94 from the theoretically predicted MDF value according to the equation:

$$96 \quad \Delta^x\text{Hg} (\%) = \delta^x\text{Hg} - \beta \times \delta^{202}\text{Hg} \quad (2)$$

where the mass-dependent scaling factor β is 0.252, 0.5024, and 0.752 for ^{199}Hg , ^{200}Hg and ^{201}Hg , respectively (Blum and Bergquist, 2007).

99

100 1.4 Backward trajectory analysis

The backward HYSPLIT trajectories of air masses at a height of 500 m above ground level and arriving at the sampling site (at 39.9725 N 116.3683 E) were simulated. Backward trajectories for each sample, ending at 1100 UTC (equal to local time 7:00 p.m.) for daytime sample and ending at 2300 UTC (equal to local time 7:00 a.m.) for nighttime sample, were calculated every 1 hrs using the Internet-Based HYSPLIT Trajectory Model and gridded meteorological data (Global Data Assimilation System, GDAS1) from the U.S. National Oceanic and Atmospheric Administration (NOAA) and were shown below (Fig. S1). The obtained average directions of arriving air masses for each sample were summarized in Table S1. The frequencies of backward trajectories were also calculated for all the samples taken during Sept. 15th to Oct. 16th 2015 using the Internet-Based HYSPLIT Trajectory Model and the archived GDAS0p5, with an interval of 3 hrs, each trajectory total run time 24 hrs and a 0.5 × 0.5 degree trajectory frequency grid resolution. The results of such simulation showed the dominating air mass arriving from southwest of the sampling site (see Fig. 1).

114

115

Table S1. List of 61 PM_{2.5} samples and their associated weather data.

Name	Sampling date	Start time	End time	Directions of arriving air mass	Weather	Sunshine duration (hrs)	SH (MJ/m ²)	O ₃ (ppbv)	T (°C)	RH (%)	MWS (m/s)	WS (m/s)
Sept-15-N	Sept-15-2015	19:02	7:02	S-SW	Cloudy			7.3	19.8	68	3.9	2
Sept-16-D	Sept-16-2015	8:25	18:55	SW	Sunny	8	6.40	67.7	24.1	52	3.9	2
Sept-16-N	Sept-16-2015	19:02	7:02	SW	Cloudy			5.6	21.1	70	3.9	2
Sept-17-D	Sept-17-2015	8:13	18:43	SW	Cloudy	4	3.02	72.3	24.8	56	4.0	2
Sept-17-N	Sept-17-2015	19:03	7:33	SW-NW	Cloudy+Rain			19.1	22.6	74	4.0	2
Sept-18-D	Sept-18-2015	8:19	18:49	N	Sunny	9	13.24	43.2	27.3	39	3.1	2
Sept-18-N	Sept-18-2015	18:57	7:27	N-NE	Clear			1.1	21.7	54	3.1	2
Sept-19-D	Sept-19-2015	8:07	18:37	NE-E	Sunny	11	17.20	41.5	26.1	33	3.6	1
Sept-19-N	Sept-19-2015	18:48	7:18	S	Clear			4.8	21.7	60	3.6	1
Sept-20-D	Sept-20-2015	8:04	18:34	SW	Cloudy	7	4.45	34.4	24.5	55	4.3	2
Sept-20-N	Sept-20-2015	18:42	7:12	SW	Cloudy			5.7	21.9	62	4.3	2
Sept-21-D	Sept-21-2015	8:17	18:47	SW	Sunny	9	6.04	41.3	25.2	49	4.1	2
Sept-21-N	Sept-21-2015	18:55	7:25	S	Cloudy			18.6	22.6	62	4.1	2
Sept-22-D	Sept-22-2015	8:18	18:18	S-SW	Overcast+Rain	0	0.43	31.4	22.9	70	5.4	2
Sept-22-N	Sept-22-2015	18:28	6:58	W-NW	Cloudy			6.3	18.3	86	5.4	2
Sept-23-D	Sept-23-2015	8:13	18:13	S-NW	Sunny	9	11.20	36.1	23.9	54	2.7	2
Sept-23-N	Sept-23-2015	18:13	6:56	S-SW	Cloudy			3.3	21.6	71	2.7	2
Sept-24-D	Sept-24-2015	8:07	18:07	S	Cloudy	2	0.73	26.5	23.0	72	3.8	2
Sept-24-N	Sept-24-2015	18:15	6:45	SE-W	Cloudy+Rain			19.4	17.7	87	3.8	2
Sept-25-D	Sept-25-2015	8:28	18:28	NW	Sunny	11	18.43	28.6	24.4	19	4.8	2
Sept-25-N	Sept-25-2015	19:03	7:33	SW-NW	Clear			1.2	17.3	44	4.8	2
Sept-26-D	Sept-26-2015	8:06	18:06	SW	Sunny	10	13.90	36.1	23.7	37	5.9	2
Sept-26-N	Sept-26-2015	18:12	6:42	SW-W	Clear			6.2	20.5	59	5.9	2
Sept-27-D	Sept-27-2015	8:21	18:21	N-NE	Sunny	10	12.56	41.9	23.8	42	3.3	2
Sept-27-N	Sept-27-2015	18:38	7:08	N-E	Cloudy			10.2	-	-	3.3	2
Sept-28-D	Sept-28-2015	8:39	18:39	E	Overcast+Rain	0	-	14.1	18.1	82	4.0	2
Sept-28-N	Sept-28-2015	18:47	7:17	E	Overcast+Rain			1.0	17.4	81	4.0	2
Sept-29-D	Sept-29-2015	8:03	18:03	E-SE	Overcast+Rain	0	-	6.7	15.7	88	3.0	2
Sept-29-N	Sept-29-2015	18:33	7:03	SE	Overcast+Rain			0.9	14.7	92	3.0	2
Sept-30-D	Sept-30-2015	8:14	18:14	SW	Cloudy+Rain	3	3.70	19.4	18.1	68	3.2	2
Sept-30-N	Sept-30-2015	18:55	7:25	SW-NW	Cloudy+Rain			13.9	15.5	67	3.2	2
Oct-1-D	Oct-1-2015	7:26	18:31	NW	Sunny	11	17.68	29.2	19.4	27	7.4	3
Oct-1-N	Oct-1-2015	18:41	7:11	NW	Clear			1.7	15.8	51	7.4	3
Oct-2-D	Oct-2-2015	8:50	18:50	NW	Sunny	11	16.00	37.6	24.3	27	4.8	2
Oct-2-N	Oct-2-2015	18:58	7:28	NW	Clear			3.2	18.4	49	4.8	2
Oct-3-D	Oct-3-2015	8:05	18:05	N-S	Sunny	10	14.35	29.1	22.5	35	4.6	2
Oct-3-N	Oct-3-2015	18:30	7:00	SW	Clear			2.1	17.7	66	4.6	2
Oct-4-D	Oct-4-2015	8:20	18:20	SW	Sunny	9	6.40	32.1	21.5	52	2.7	1
Oct-4-N	Oct-4-2015	18:44	7:14	SW	Clear			1.4	17.9	74	2.7	1
Oct-5-D	Oct-5-2015	8:03	18:03	SW	Haze	6	3.89	51.6	21.8	59	3.0	1
Oct-5-N	Oct-5-2015	19:04	7:34	SW	Haze			2.8	18.3	83	3.0	1
Oct-6-D	Oct-6-2015	8:24	18:24	SW-W	Haze	5	3.03	71.4	23.0	60	2.7	1
Oct-6-N	Oct-6-2015	19:25	7:25	SW	Haze			3.4	19.8	81	2.7	1
Oct-7-D	Oct-7-2015	7:55	16:55	SW-NW	Haze	2	1.66	31.6	22.6	68	3.4	2
Oct-7-N	Oct-7-2015	18:00	6:00	NW	Clear			18.9	19.1	24	3.4	2
Oct-8-D	Oct-8-2015	8:07	18:07	NW	Sunny	11	16.11	24.9	17.8	15	7.1	3
Oct-8-N	Oct-8-2015	18:43	6:43	NW	Clear			2.6	14.3	31	7.1	3
Oct-9-D	Oct-9-2015	7:43	17:13	NW	Sunny	11	12.81	18.1	18.7	20	8.3	4
Oct-9-N	Oct-9-2015	17:53	5:23	NW-N	Cloudy			17.9	12.5	30	8.3	4
Oct-10-D	Oct-10-2015	8:10	18:10	NW-N	Sunny	10	12.75	23.8	14.4	24	7.7	4
Oct-10-N	Oct-10-2015	18:38	7:08	N	Cloudy			23.3	15.3	27	7.7	4
Oct-11-D	Oct-11-2015	8:35	18:00	N	Sunny	10	12.63	30.4	20.1	26	7.1	3
Oct-11-N	Oct-11-2015	18:08	6:38	N	Cloudy			5.8	16.6	27	7.1	3
Oct-12-D	Oct-12-2015	7:49	17:31	NW	Sunny	11	14.67	27.4	22.5	20	5.9	1
Oct-12-N	Oct-12-2015	17:40	6:10	NW	Cloudy			2.7	17.8	34	5.9	1
Oct-13-D	Oct-13-2015	8:26	17:48	NW-W	Sunny	11	13.84	22.4	23.7	22	3.7	1
Oct-13-N	Oct-13-2015	17:53	6:23	SW-SE	Cloudy			1.3	17.2	50	3.7	1
Oct-14-D	Oct-14-2015	8:17	17:47	S-E	Cloudy	4	2.99	12.4	20.1	45	3.5	2
Oct-14-N	Oct-14-2015	17:53	6:23	SW-NW	Cloudy			1.1	16.3	64	3.5	2
Oct-15-D	Oct-15-2015	8:28	17:33	W-NW	Sunny	9	8.31	31.9	22.5	38	3.1	2
Oct-15-N	Oct-15-2015	17:39	6:09	W	Cloudy			3.3	19.7	55	3.1	2

117 SH is the daily solar radiation on a horizontal surface, T is 12-hour averaged temperature, RH is 12-hour averaged relative humidity, MWS is the daily (24-hour) maximum wind speed, and WS is the daily average wind speed.

120 **Table S2.** Contents of PM_{2.5}, Hg in PM_{2.5} (PM_{2.5}-Hg) and Hg isotopic composition of PM_{2.5}-
121 Hg.

Name	PM _{2.5} ($\mu\text{g}/\text{m}^3$)	Hg Con. ($\mu\text{g}/\text{g}$)	$\delta^{202}\text{Hg}$ (‰)	2SD	$\Delta^{199}\text{Hg}$ (‰)	2SD	$\Delta^{200}\text{Hg}$ (‰)	2SD	$\Delta^{201}\text{Hg}$ (‰)	2SD
Sept-15-N	85	0.52	-0.89	0.14	0.05	0.06	0.13	0.04	-0.08	0.07
Sept-16-D	71	0.41	-0.61	0.14	0.30	0.06	0.06	0.04	0.05	0.07
Sept-16-N	88	0.44	-0.53	0.14	-0.05	0.06	0.06	0.04	-0.11	0.07
Sept-17-D	76	0.38	-0.47	0.14	0.21	0.06	0.01	0.04	0.08	0.07
Sept-17-N	94	0.47	-0.27	0.14	-0.08	0.06	0.03	0.04	-0.15	0.07
Sept-18-D	32	0.17	-0.72	0.14	0.90	0.06	0.08	0.04	0.64	0.07
Sept-18-N	43	0.31	-1.29	0.14	0.04	0.06	-0.02	0.04	-0.12	0.09
Sept-19-D	13	0.09								
Sept-19-N	52	0.29	-0.98	0.14	0.09	0.06	0.02	0.04	-0.06	0.07
Sept-20-D	63	0.61	-0.48	0.14	0.16	0.06	0.12	0.04	0.02	0.07
Sept-20-N	63	0.89	-0.59	0.14	0.01	0.06	0.04	0.04	0.06	0.07
Sept-21-D	61	0.48	-0.34	0.14	0.50	0.06	0.05	0.04	0.34	0.07
Sept-21-N	83	0.62	-0.69	0.14	0.10	0.06	0.06	0.04	0.07	0.07
Sept-22-D	95	0.53	-0.40	0.14	0.28	0.06	0.03	0.04	0.18	0.07
Sept-22-N	23	0.31	-0.83	0.14	-0.06	0.06	-0.01	0.04	-0.09	0.07
Sept-23-D	19	0.15								
Sept-23-N	39	0.54	-0.87	0.14	0.17	0.06	0.03	0.04	0.09	0.07
Sept-24-D	84	0.38	-0.25	0.14	0.02	0.06	0.11	0.04	0.03	0.07
Sept-24-N	47	0.20	-0.47	0.14	0.05	0.06	0.06	0.04	-0.11	0.07
Sept-25-D	9	0.38	-0.49	0.14	0.21	0.06	0.18	0.04	0.21	0.07
Sept-25-N	33	0.14	-0.57	0.14	0.42	0.06	0.08	0.04	0.27	0.07
Sept-26-D	24	0.20	-0.37	0.14	1.04	0.06	0.10	0.04	0.71	0.07
Sept-26-N	51	0.44	-0.64	0.18	0.30	0.06	0.09	0.04	0.17	0.07
Sept-27-D	31	0.39	-0.30	0.14	0.76	0.06	0.12	0.04	0.61	0.07
Sept-27-N	46	0.78	-0.62	0.14	0.15	0.06	0.07	0.04	0.08	0.07
Sept-28-D	34	0.32	-0.38	0.14	-0.48	0.06	0.02	0.04	-0.52	0.07
Sept-28-N	34	0.34	-0.32	0.14	-0.46	0.06	0.01	0.04	-0.45	0.07
Sept-29-D	52	0.48	0.29	0.14	0.06	0.06	0.20	0.04	0.26	0.09
Sept-29-N	13	0.36	-0.82	0.14	-0.04	0.06	0.02	0.04	-0.03	0.07
Sept-30-D	14	0.16	-0.23	0.14	-0.13	0.06	0.16	0.04	-0.14	0.07
Sept-30-N	22	0.64	-0.26	0.14	-0.04	0.06	0.08	0.04	-0.05	0.07
Oct-1-D	7	0.12								
Oct-1-N	19	0.67	-0.91	0.14	0.11	0.06	0.11	0.04	0.09	0.07
Oct-2-D	18	0.20	-0.54	0.14	0.29	0.06	0.14	0.04	0.26	0.07
Oct-2-N	31	0.59	-1.49	0.14	0.13	0.06	-0.02	0.04	0.18	0.07
Oct-3-D	19	0.26	-0.21	0.14	0.86	0.06	0.21	0.04	0.59	0.07
Oct-3-N	39	0.59	-0.95	0.14	0.18	0.06	0.07	0.04	0.20	0.07
Oct-4-D	88	0.36	-0.80	0.14	0.27	0.06	0.02	0.04	0.09	0.07
Oct-4-N	119	0.38	-0.97	0.14	-0.11	0.06	0.02	0.04	-0.16	0.07
Oct-5-D	114	0.37	-0.32	0.14	-0.53	0.06	0.09	0.04	-0.64	0.07
Oct-5-N	138	0.53	-0.69	0.14	-0.51	0.06	0.06	0.04	-0.54	0.07
Oct-6-D	156	0.39	-0.09	0.14	-0.40	0.06	0.08	0.04	-0.57	0.07
Oct-6-N	158	0.44	0.16	0.14	-0.15	0.06	0.10	0.04	-0.12	0.07
Oct-7-D	138	0.47	0.20	0.14	0.69	0.06	0.08	0.04	0.42	0.07
Oct-7-N	128	0.46	0.52	0.14	0.55	0.06	0.14	0.04	0.39	0.07
Oct-8-D	4	0.30	-0.22	0.14	0.32	0.06	0.19	0.04	0.20	0.07
Oct-8-N	16	0.24	0.55	0.14	-0.07	0.06	0.09	0.04	0.01	0.07
Oct-9-D	24	0.43	-0.47	0.14	0.04	0.06	0.07	0.04	0.12	0.07
Oct-9-N	17	0.08								
Oct-10-D	14	0.19	-0.82	0.14	0.33	0.06	0.08	0.04	0.55	0.07
Oct-10-N	8	0.26	-0.61	0.14	0.32	0.06	0.11	0.04	0.28	0.07
Oct-11-D	12	0.10								
Oct-11-N	15	0.38	-0.42	0.14	0.17	0.06	0.14	0.04	0.20	0.07
Oct-12-D	10	0.27	-0.79	0.14	0.28	0.06	0.12	0.04	0.27	0.07
Oct-12-N	26	1.22	-0.90	0.14	-0.03	0.06	0.05	0.04	-0.03	0.07
Oct-13-D	19	0.43	-0.70	0.14	0.23	0.06	0.01	0.04	0.16	0.07
Oct-13-N	60	0.89	-0.80	0.14	-0.01	0.06	0.06	0.04	-0.06	0.07
Oct-14-D	50	0.37	-0.78	0.14	0.01	0.06	-0.01	0.04	0.00	0.07
Oct-14-N	82	0.49	-1.21	0.14	-0.20	0.06	-0.02	0.04	-0.18	0.07
Oct-15-D	50	0.34	-0.60	0.14	0.57	0.06	0.08	0.04	0.52	0.07
Oct-15-N	95	0.33	-0.37	0.14	0.21	0.06	0.07	0.04	0.33	0.07

123 **Table S3.** The below results of Paired Samples T-Test and Independent Samples T-Test were
 124 obtained using the IBM SPSS Statistics Version 22. The paired samples were consecutive day
 125 and night PM_{2.5} samples, for example, Sept-16-D and Sept-16-N were paired samples.

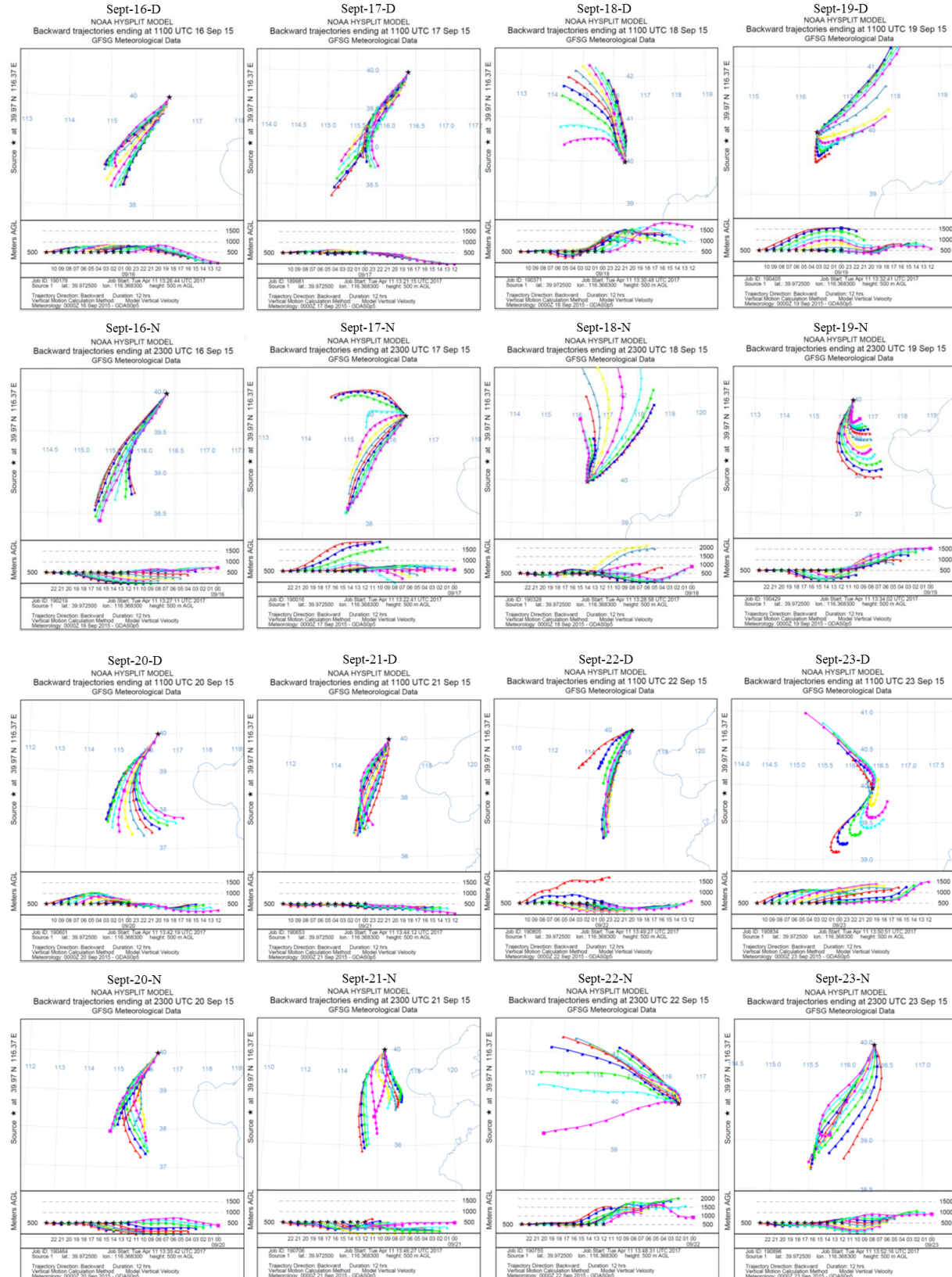
Paired Samples Test											
Day - Night	Paired Differences					t	df	Sig. (2-tailed)			
	Mean	Std. Deviation	Std. Error Mean	95% Confidence Interval of the Difference							
				Lower	Upper						
PM _{2.5}	-2.06667	78.67959	14.36486	-31.44611	27.31278	-0.144	29	0.887			
Hg Con.	-0.15263	0.27183	0.04963	-0.25414	-0.05113	-3.075	29	0.005			
δ ²⁰² Hg	0.16960	0.41413	0.08283	-0.00134	0.34054	2.048	24	0.052			
Δ ¹⁹⁹ Hg	0.24400	0.28384	0.05677	0.12684	0.36116	4.298	24	0.000			
Δ ²⁰⁰ Hg	0.04120	0.06412	0.01282	0.01473	0.06767	3.213	24	0.004			

126

Independent Samples Test							
Day vs Night	Mean Difference	Std. Error Difference	95% Confidence Interval of the Difference		t	df	Sig. (2-tailed)
			Lower	Upper			
PM _{2.5}	-2.57742	22.46315	-47.52607	42.37123	-0.115	59	0.909
Hg Con.	-0.15408	0.04966	-0.25393	-0.05423	-3.103	47.858	0.003
δ ²⁰² Hg	0.20549	0.10385	-0.00272	0.41370	1.979	54	0.053
Δ ¹⁹⁹ Hg	0.21982	0.08777	0.04209	0.39755	2.505	37.666	0.017
Δ ²⁰⁰ Hg	0.03464	0.01437	0.00582	0.06346	2.410	54	0.019

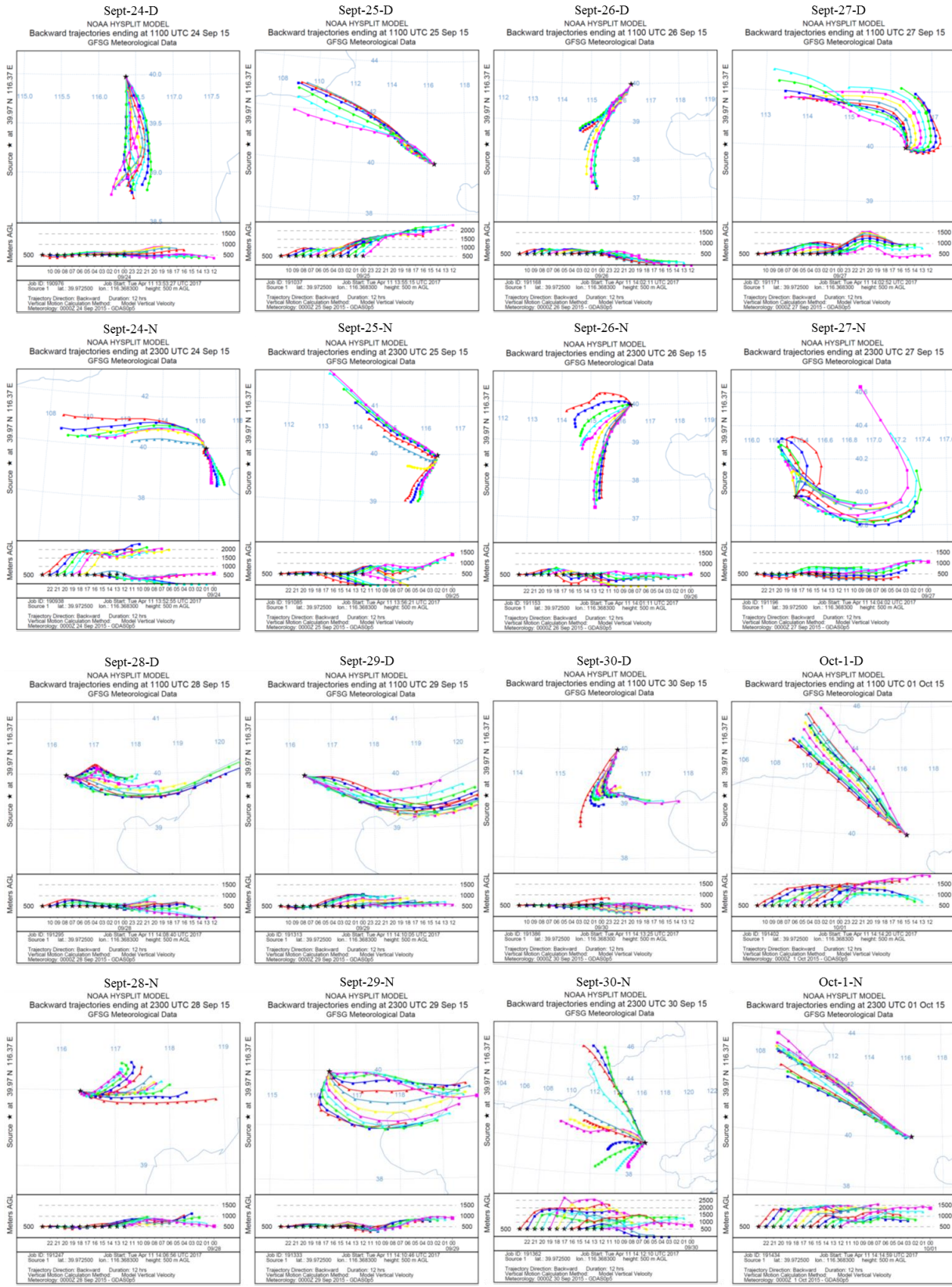
127

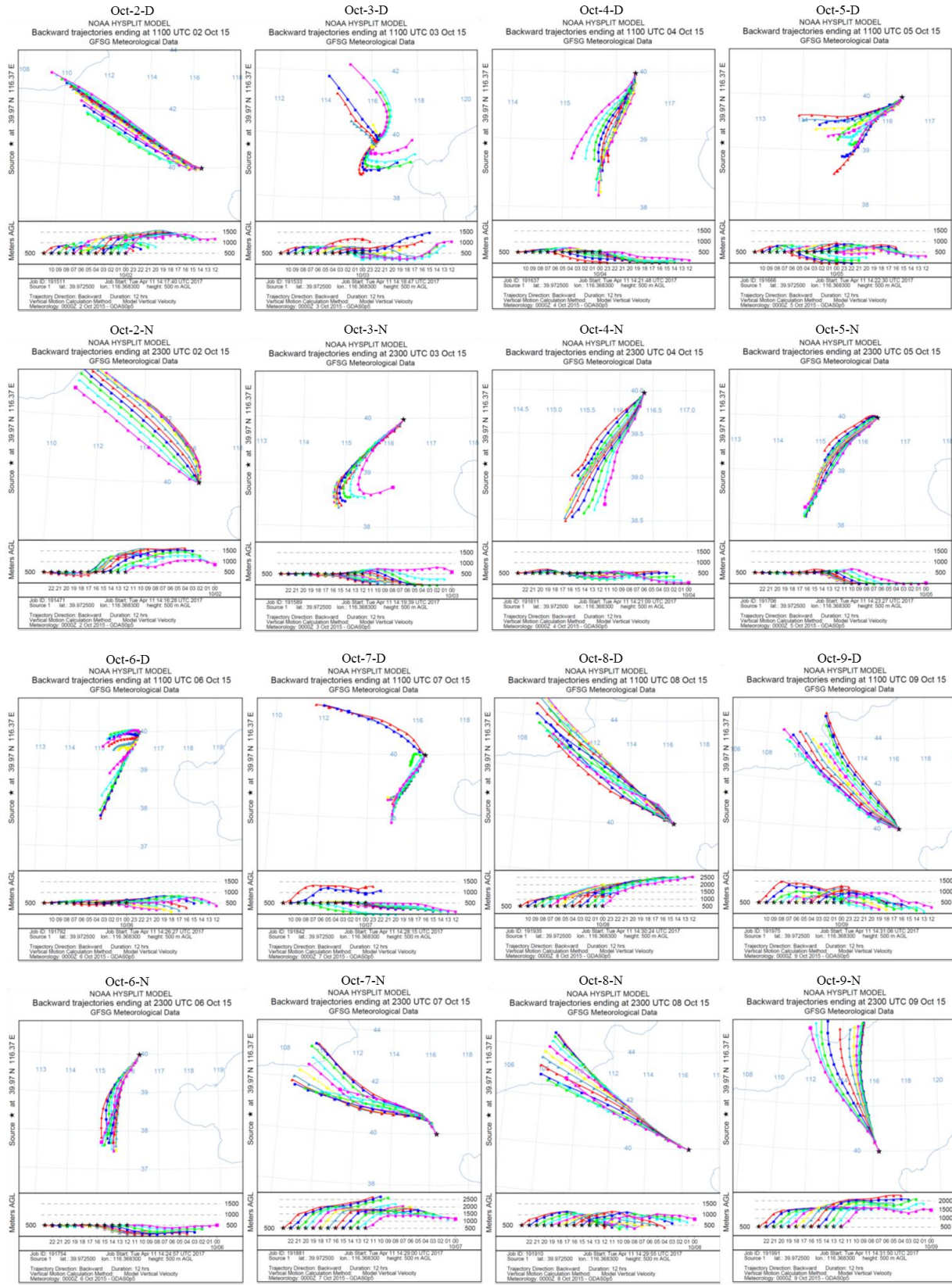
128 **Figure S1.** NOAA-HYSPLIT model shown back trajectories for 30 day-night PM_{2.5} sample
 129 pairs collected during Sep. 16th to Oct. 15th 2015 from urban center of Beijing, China. Arriving
 130 air masses of 500 m above ground level (AGL) were calculated on website of
 131 <http://ready.arl.noaa.gov/hypub-bin/trajtype.pl?runtype=archive>.



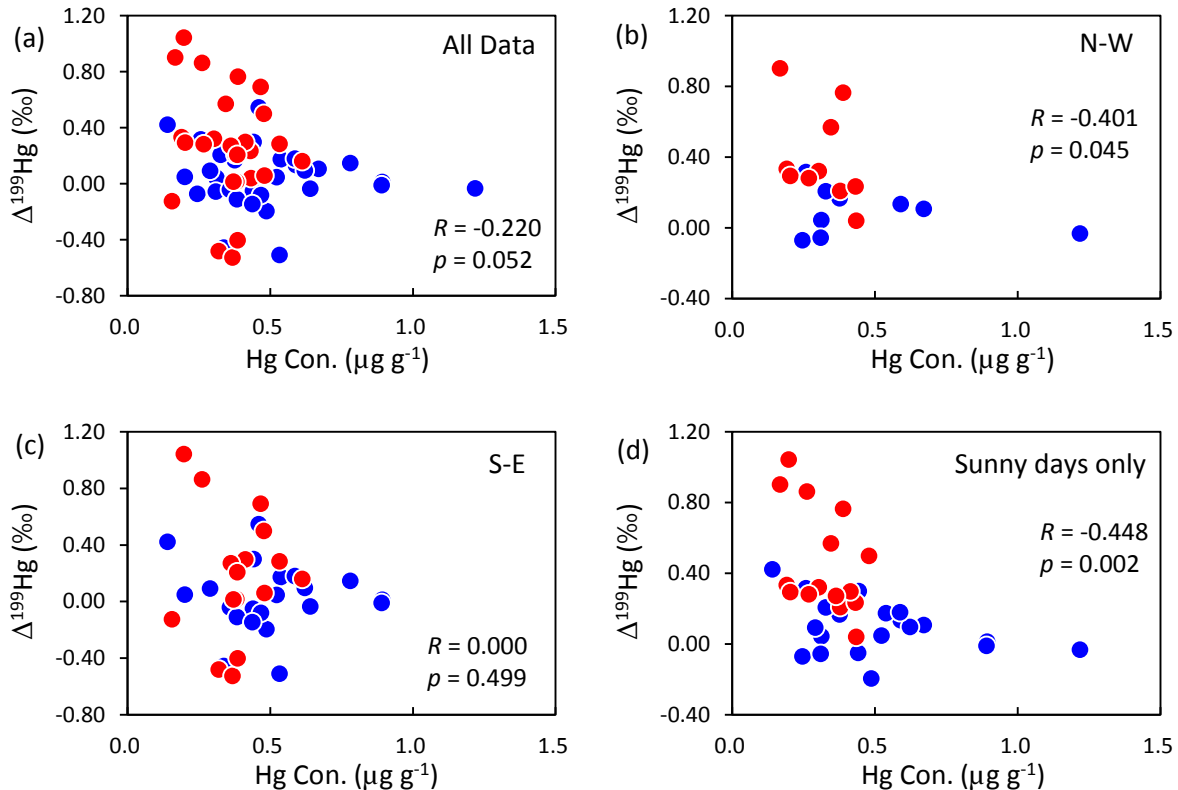
132

133





140 **Figure S2.** $\Delta^{199}\text{Hg}$ (%) versus the content of Hg in PM_{2.5} ($\mu\text{g g}^{-1}$) for different subsets of PM_{2.5}
141 samples: a) all data, b) North-West (N-W), c) South-East (S-E) and d) All sunny days (Sun),
142 with Spearman Correlation Coefficient (R) and 1-tailed significant (p). The red circles are for
143 daytime samples, while blue circles are for night samples.

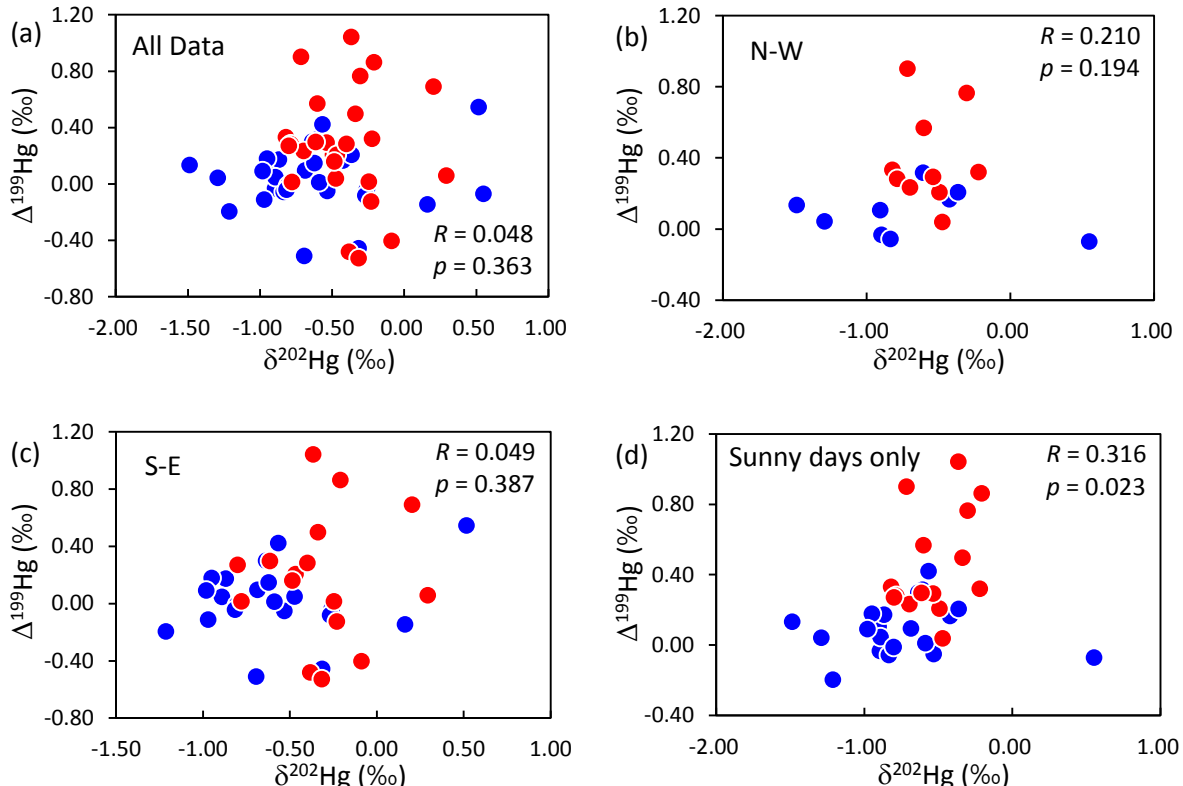


144

145

146

147 **Figure S3.** $\Delta^{199}\text{Hg}$ (‰) versus $\delta^{202}\text{Hg}$ (‰) for different subsets of PM_{2.5} samples: a) all data, b)
148 North-West (N-W), c) South-East (S-E) and d) All sunny days (Sun), with Spearman
149 Correlation Coefficient (R) and 1-tailed significant (p). The red circles are for daytime
150 samples, while the blue circles are for night samples.

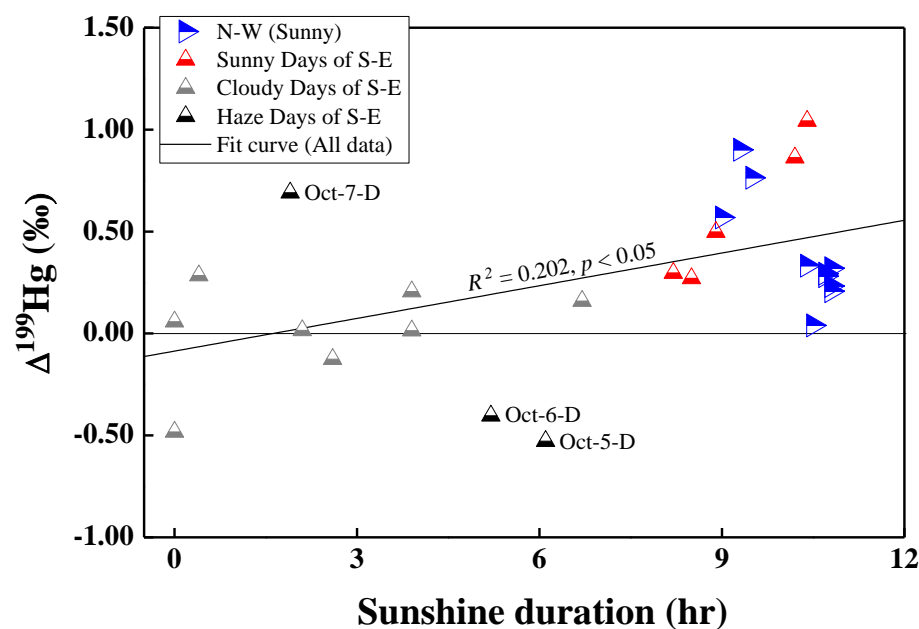


151

152

153

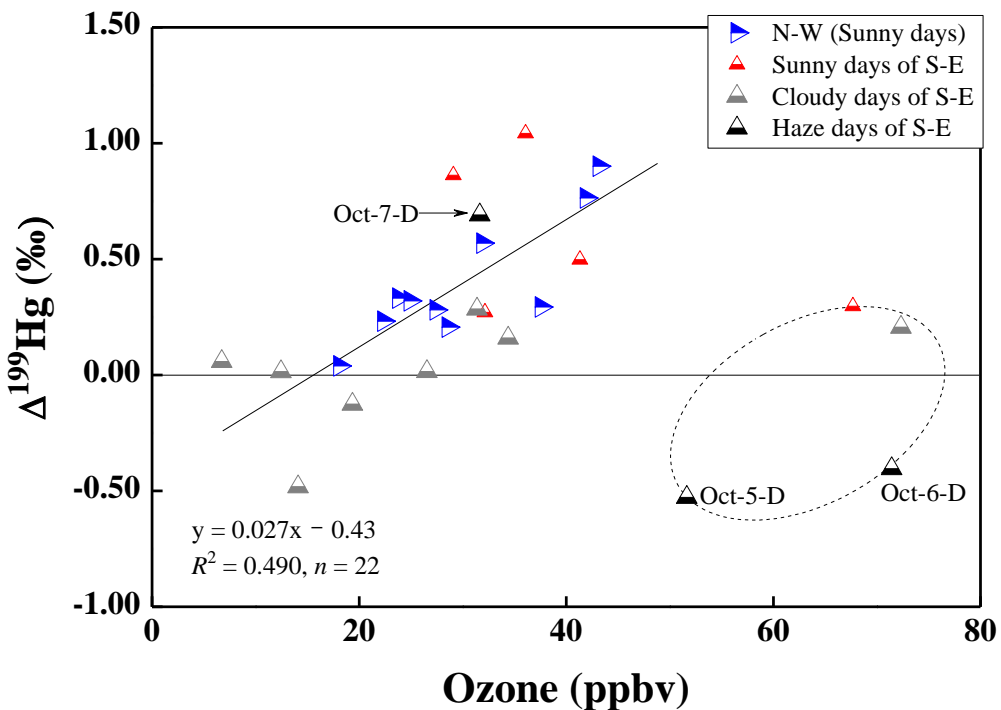
154 **Figure S4.** $\Delta^{199}\text{Hg}$ values of daytime PM_{2.5} samples versus sunshine duration (hr).



155

156

157 **Figure S5.** $\Delta^{199}\text{Hg}$ values of daytime PM_{2.5} samples versus atmospheric ozone content (ppbv).

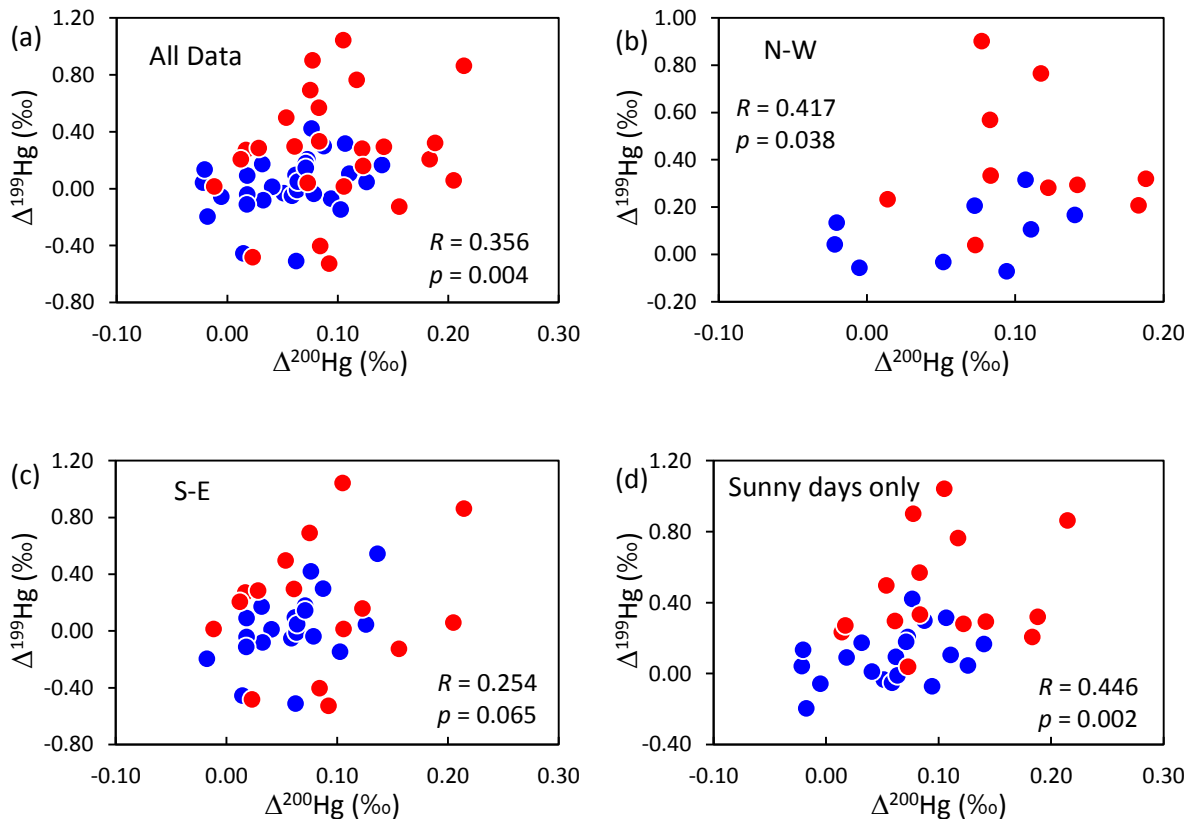


158

159

160 **Figure S6.** $\Delta^{199}\text{Hg}$ (‰) versus $\Delta^{200}\text{Hg}$ (‰) for different subsets of PM_{2.5} samples: a) all data,
 161 b) North-West (N-W), c) South-East (S-E) and d) All sunny days (Sun). The red circles are
 162 for daytime samples, while the blue circles are for night samples. Positive correlations
 163 between $\Delta^{199}\text{Hg}$ and $\Delta^{200}\text{Hg}$ can be seen in each subsets, with Spearman Correlation
 164 Coefficient (R) and 1-tailed significant (p).

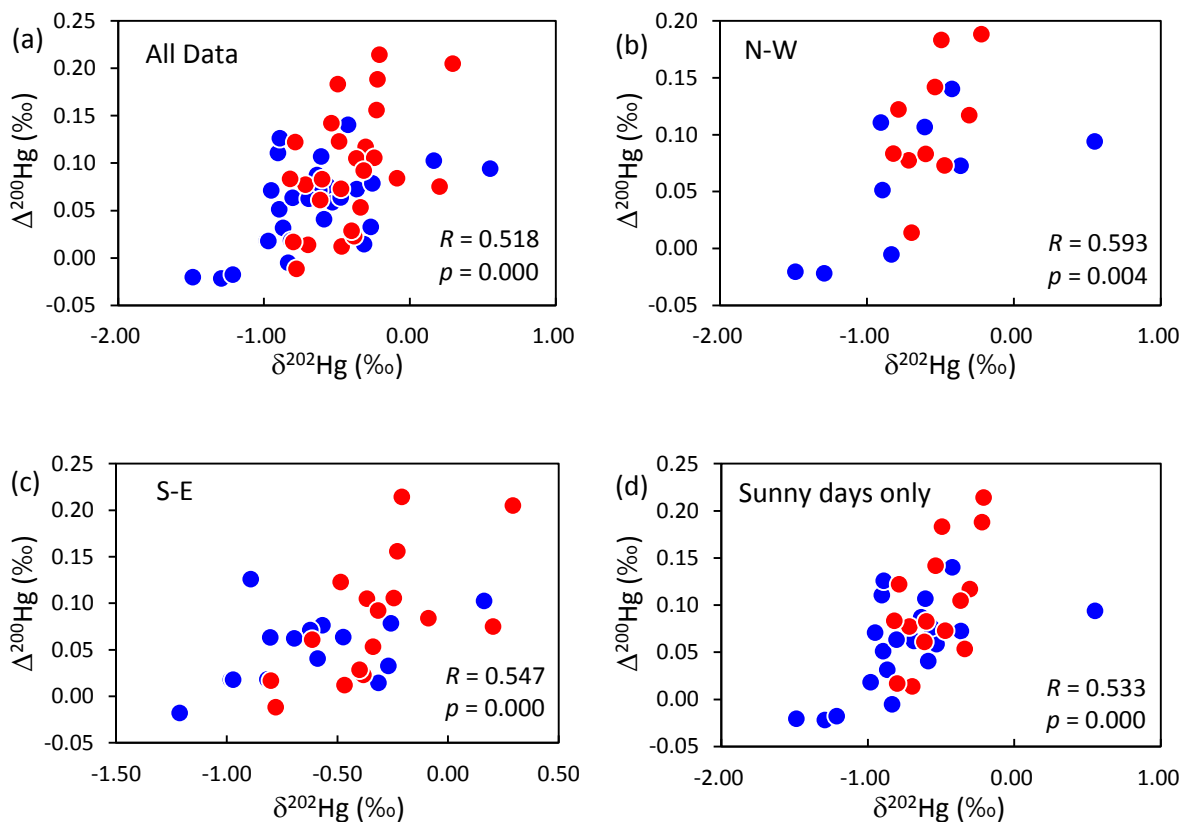
165



166

167

168 **Figure S7.** $\Delta^{200}\text{Hg} (\text{\textperthousand})$ versus $\delta^{202}\text{Hg} (\text{\textperthousand})$ for different subsets of PM_{2.5} samples: a) all data, b)
 169 North-West (N-W), c) South-East (S-E) and d) All sunny days (Sun). The red circles are for
 170 daytime samples, while the blue circles are for night samples. Positive correlations between
 171 $\Delta^{200}\text{Hg}$ and $\delta^{202}\text{Hg}$ can be seen in each subsets with Spearman Correlation Coefficient (R) and
 172 1-tailed significant (p).



173

174

175

176 **REFERENCES**

- 177 Blum, J. D., and Bergquist, B. A.: Reporting of variations in the natural isotopic composition
178 of mercury, *Anal. Bioanal. Chem.*, 388, 353-359, 2007.
- 179 Huang, Q., Liu, Y. L., Chen, J. B., Feng, X. B., Huang, W. L., Yuan, S. L., Cai, H. M., and Fu,
180 X. W.: An improved dual-stage protocol to pre-concentrate mercury from airborne
181 particles for precise isotopic measurement, *J. Anal. At. Spectrom.*, 30, 957-966, 2015.
- 182 Huang, Q., Chen, J., Huang, W., Fu, P., Guinot, B., Feng, X., Shang, L., Wang, Z., Wang, Z.,
183 Yuan, S., Cai, H., Wei, L., and Yu, B.: Isotopic composition for source identification of
184 mercury in atmospheric fine particles, *Atmos. Chem. Phys.*, 16, 11773-11786, 2016.

185